Simulation of Intra-operative 3D Coronary Angiography for Enhanced Minimally Invasive Robotic Cardiac Intervention

G. Lehmann, D. Habets, D.W. Holdsworth, T. Peters, and M. Drangova

The John P Robarts Research Institute, The University of Western Ontario
and the London Health Sciences Centre. London Ontario, Canada

Abstract. A simulation environment has been developed to aid the development of three-dimensional (3D) angiographic imaging of the coronary arteries for use during minimally invasive robotic cardiac surgery. We have previously developed a dynamic model of the coronary arteries by non-linearly deforming a high-resolution 3D image of the coronaries of an excised human heart, based on motion information from cine bi-plane angiograms. The result was a sequence of volumetric images representing the motion of the coronary arteries throughout the cardiac cycle. To simulate different acquisition and gating strategies, we implemented an algorithm to forward project through the volume data sets. Thus, radiographic projections corresponding to any view-angle, can be produced for any time-point throughout the cardiac cycle. Combining re-projections from selected time-points and view angles enables the evaluation of various gating strategies. This approach will allow us to determine the optimum image acquisition parameters to produce 3D coronary angiograms for planning and guidance of minimally invasive robotic cardiac surgery.

1 Introduction

Traditional coronary artery bypass (CAB) procedures create an alternate route of blood supply, bypassing an occluded artery by grafting a vessel from another part of the body. CAB procedures require a full sternotomy and cardio-pulmonary bypass, each of which inflict significant trauma to the patient and require a lengthy recovery period. To decrease the associated trauma of CAB procedures, minimally invasive direct CAB (MIDCAB) and more recently, minimally invasive robotic CAB (MIRCAB) have been implemented.

MIDCAB techniques eliminate the need for full sternotomy and cardio-pulmonary bypass and are all performed on the beating heart with endoscopic port-access inserted through a small incision in the chest wall. A major limitation of MIDCAB is that the long-handled instruments magnify hand tremors, which can make precise suturing difficult and tiring.

Robot-assisted surgical systems were developed for MIRCAB to avoid the restrictions of conventional endoscopic port-access instruments, to remove surgeon tremor,

T. Dohi and R. Kikinis (Eds.): MICCAI 2002, LNCS 2489, pp. 268–275, 2002.

provide a minification factor between the operator's movements and the tools, and permit the surgeon to perform the procedure from a comfortable position. MIRCAB procedures have several technical limitations, including the lack of guidance from conventional two-dimensional (2D) images of patients, possible improper port placement and limited field of view of the operative site from the endoscope. These problems are being addressed by a virtual cardiac surgical planning (VCSP) platform [1,2] being developed at the John P. Robarts Research Institute. The VCSP will ultimately provide the surgeon with a dynamic, virtual representation of the patient's thorax in the operating room where the patient's heart motion and positioning are synchronized in the virtual environment. With such a system, the surgeon would always maintain a global view of the operative site, and not be constrained by the small field-of-view of the endoscope.

We believe that further improvements in the MIRCAB procedure could result from pre- and intra-procedure three-dimensional (3D) angiograms of the coronary arteries. Since the heart is beating during an interventional procedure, intra-operative 3D coronary angiograms could be used to update preoperative images in the VCSP to verify the location of the surgical instruments with respect to the surgical target, as well as to verify, post-operatively a successful bypass graft. Recent advances in cone-beam CT - including computed rotational angiography (CRA, also known as 3D DSA, Cone-beam C-arm CT, etc), [3,4] electro-cardiograph (ECG) gating strategies, and the potential for fast CCD-equipped x-ray image intensifiers (XRII) - warrant a feasibility study into the implementation of 3D coronary angiography in the operating room.

We have begun a preliminary investigation aimed at providing intra-operative 3D coronary angiography by modifying a clinical C-arm angiography system in the operating room. The purpose of this paper is to demonstrate the capability of a numerical modeling environment to simulate acquisition and gating strategies and how they will be used to investigate the feasibility of intra-operative 3D coronary angiography.

2 Methods

The human heart is relatively still during the diastolic phase of the cardiac cycle, making it possible to select projections during diastole and reconstruct a 3D volume with acceptable artifacts arising from cardiac motion. The simulation environment uses a dynamic 3D model of the coronary circulation to investigate the appropriate projections that can be selected from diastole. To allow a comparison of image quality, the numerical simulation environment mimics the imaging parameters of a CRA system, thus allowing simulated images to be compared to the images acquired with the CRA system.

2.1 Dynamic Model of the Coronary Circulation

We have previously developed a realistic dynamic model of the coronary circulation [5] and briefly outline the essential steps in the following section. The dynamic coronary artery model was developed from high-quality 3D CT images of static human coronary arteries and cine bi-plane angiograms from a patient with similar coronary anatomy, as described below.

2.1.1 High Quality 3D CT Image of Human Coronary Arteries

A modified clinical angiography system [3,4] that was developed for cerebrovascular procedures was used to obtain a 3D CT image of coronary arteries in a human cadaver heart that was clamped at the aortic root and cannulated. To equalize the x-ray attenuation path throughout the myocardium and its environment the heart was suspended in a saline bath and perfused with saline solution. Iodinated contrast agent was injected manually into the aortic root, providing adequate contrast for imaging the coronary arteries. Acquisition of 2D projections over 200^{o} (30-Hz acquisition rate at 90-kVp and 2-mAs with a nominal field of view of 28-cm) commenced when the coronary arteries were filled with contrast agent and the contrast-agent injection continued throughout the 4.5-s acquisition. From the 129 acquired projections, a 400x400x400 volumetric image of the coronary arteries, with 400-μm isotropic voxels was reconstructed.

2.1.2 3D Motion Information from 2D Bi-plane Angiograms

Based on the 3D CT image of the coronary, a cardiac patient with coronary anatomy similar to that of the excised heart was selected. The patient was imaged using a clinical bi-plane angiography system using the standard right anterior oblique (RAO) and left anterior oblique (LAO) geometries for imaging the coronaries. To determine the motion of the coronary arteries in 2D, arterial bifurcations were used as landmarks that could be followed throughout the cardiac cycle.

To find the 3D distribution of the bifurcations identified in the LAO and RAO images, the imaging system was calibrated using a phantom containing eleven 1.5-mm diameter steel spheres. The 3D coordinates of the vascular landmarks were then determined using standard least-squares techniques. This procedure was repeated at successive intervals throughout the cardiac cycle, resulting in a series of volumes that tracked the dynamically changing 3D coordinates of the landmarks. From these coordinates, a dynamic set of vectors that describe the motion of the vascular landmarks throughout the cardiac cycle was constructed.

2.1.3 Non-linear Deformation

This set of dynamic vectors was then used to drive a thin-plate-spline [6] based non-linear warping algorithm to deform the 3D static image of the coronary arteries between time points in the cardiac cycle. For the purposes of the work presented here, the point constraints used in the non-linear warping algorithm are the bifurcation landmarks identified on the 3D CT image and the corresponding landmarks (typically 18) determined from the cine bi-plane images.

The image analysis software used to create the coronary-artery model consisted of Python applications based on the Visualization Toolkit (VTK) libraries. The non-linear deformation algorithm, contained in the VTK libraries was implemented based on the 3D motion of the landmarks. Each deformation was performed with respect to the original 3D CT image to minimize the image degradation associated with successive deformations.

The resulting dynamic model consisted of 26-temporal volumes with a frame rate of 30-Hz, the model therefore represents a patient with a 69-bpm heart rate. The implementation utilized C++ classes and Python [7,8] applications based on the Visualization Toolkit (VTK) [9] libraries. The methods described in the following sections were also implemented in VTK.

2.2 3D Coronary Angiography Simulation Environment

To be able to simulate different gating strategies within the 3D-coronary angiography simulation environment, we implemented a ray-driven projection method to generate angiographic views at arbitrary angles. For each ray passing through the model the values are summed to create a simulated radiographic projection. Note that unlike the projections obtained using the XRII-based detector of the CRA system, which represents variations in x-ray intensity, our algorithm calculates the sum of the linear attenuation coefficients along the path of each ray. This allows the calculated projections to be reconstructed without further image processing.

The forward-projection algorithm used is based on a method [10] that considers the CT data to consist of the intersection volumes of three orthogonal sets of equally spaced, parallel planes. This algorithm scales to 3N with the number of planes, rather than previously-proposed projection algorithms which scale to N^3, where N is the number of voxels in the 3D CT data set. The forward-projection algorithm simulated the geometric parameters of the CRA system. Projection views, within a 200° span are simulated from volumes representing the different phases of the cardiac cycle, and combined to produce complete sets of raw projection data. The projections were reconstructed using a modified Feldkamp cone-beam algorithm [11].

2.3 Preliminary Simulation of Prospectively Gated Acquisition

For cardiac imaging, the acquisition must to be synchronized to the cardiac cycle. Since the heart moves relatively little during diastole, it is possible to combine projections obtained at any time point during diastole as if the heart was stationary throughout that time period. To demonstrate the utility of the simulation environment, we preformed a preliminary study focused on determining the effect of reducing the number of views used in the reconstruction of a 3D coronary artery image and the amount of motion that can be tolerated during image acquisition.

First, the effect of a reduced the number of views was investigated by reconstructing a 3D image from 129 (the number of views used to reconstruct the original CT image of the excised human heart), 65 and 33 views. For this test all views were obtained from the original static CT image of the excised human heart, thereby not introducing artifacts due to cardiac motion.

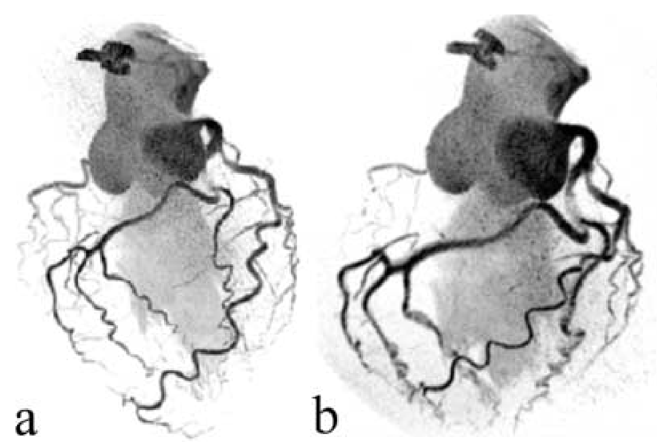

Fig. 1. Comparison of the original CT image to simulated CT. (a) MIP through the original volume (b) MIP through the simulated volume. Note that the heart is viewed at slightly different angles in (a) and (b).

The numerical environment was then used to simulate different acquisition and gating strategies. In these simulations, it was assumed that projections are collected at known view angles over a predetermined fraction of the cardiac cycle. A 30-Hz acquisition rate was assumed, mimicking the current acquisition rate of the CRA. In the simulation environment this parameter can be increased to model systems equipped with faster CCD cameras. Our preliminary study investigated two acquisition strategies: (I) consecutive views are acquired over a 200-ms acquisition window during a pre-selected time point in the cardiac cycle and multiple cardiac cycles are used to complete the acquisition of views over 200°, and (II) the same strategy implemented with a 100-ms acquisition window. For each of these strategies the number of views obtained per cardiac cycles depends on the length of the acquisition window and the frame rate of the imaging system; thus for strategy (I) 6 views are acquired per cycle and for strategy (II) 3 views are obtained. Both of these strategies were evaluated with a varying number of views, ranging between 65 and 129. Finally, the time-point in the cardiac cycle, about which the acquisition window is centered, was varied from early to mid diastole.

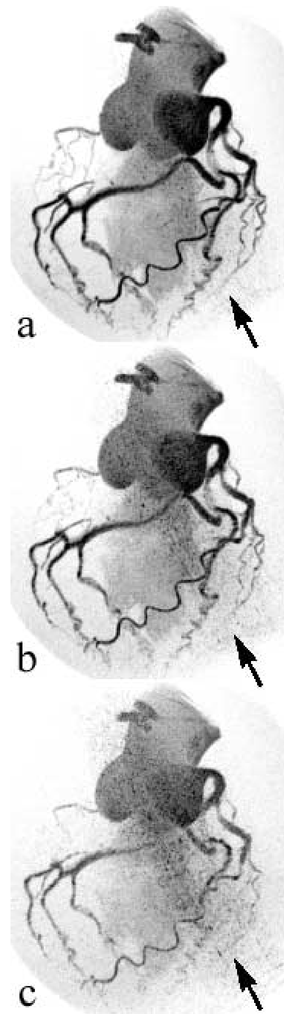

Fig. 2. The effect of a decreased number of views on 3D coronary angiography with arrows indicating the decreased detail in smaller coronary vessels. Shown are (a) MIP of the simulated volume reconstructed using 129 views (b) MIP reconstructed using 65 views and (c) MIP reconstructed using 33 views.

3 Results

To demonstrate numerical simulation of 3D coronary angiography we have shown a maximum intensity projection (MIP), Fig. 1a of an excised human heart acquired with a CRA system and a MIP, Fig. 1b of a simulated CT image. The simulated CT image was created by the numerical environment using Fig. 1a as the input, re-projecting 129 view angles over 200° through the volume by mimicking the CRA parameters and reconstructing the simulated projections.

The effect of a decreased number of views on 3D coronary angiography was investigated and the results are shown in Fig. 2. Figure 2a is identical to Fig. 1b, the simulated 3D coronary angiogram reconstructed using 129 views. To demonstrate the effect of a decreased number of views simulated angiograms were reconstructed using 65 views (Fig. 2b) and 33 views (Fig. 2c). The arrows in Fig. 2 show the decrease in detail of the smaller coronary vessels going from (a) to (c). The decreased contrast-to-noise ratio in the images is due to the decreased number of views.

Gating strategies (I) and (II) were implemented using the dynamic model during the i) early and ii) mid diastole phases of the cardiac cycle. Figure 3 shows the result of gating strategy (I), acquired using a 200-ms acquisition window. Figures 3a,b show MIPs through the images created in early diastole, and similarly Figs. 3c,d show MIPs obtained through volumes reconstructed from projections acquired during mid diastole. Figures 3a-c and Figs. 3b,d were created using 129 views (or 22 cardiac cycles x 6 views per cardiac cycle) and 65 views, which corresponds to 22 cardiac cycles and 11 cardiac cycles, respectively.

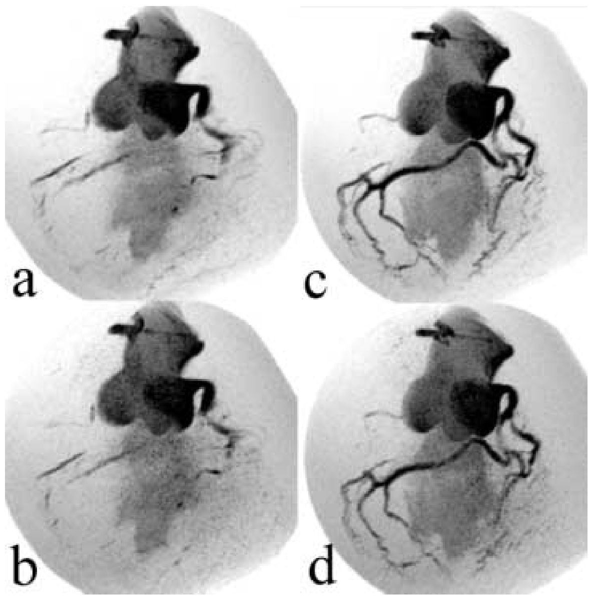

Fig. 3. MIPs through the volumes created using gating strategy (I), a 200-ms acquisition window. Shown are (a) 129 views, and (b) 65 views acquired during early diastole, and (c) 129 views, and (d) 65 views acquired during mid diastole.

The effects of cardiac motion are seen Figs. 3a,b, where the heart was moving too rapidly at the end of systole and the beginning of diastole to acquire 3D coronary angiograms of sufficient quality. Figures 3c,d, acquired during mid diastole show improved image quality. The heart was relatively stationary during the mid diastole acquisition showing that a reasonable 3D coronary angiogram can be acquired in 11 cardiac cycles, Fig. 3d.

Figure 4 shows the result of gating strategy (II), acquired using a 100-ms acquisition window. Figures 4a,b show MIPs through the images created in early diastole, and similarly Fig. 4c,d show the mid diastolic phase of the cardiac cycle. Figure 4a,c and Figs. 4b,d were created using 129 views and 65 views, which corresponds to 43 cardiac cycles and 22 cardiac cycles respectively.

The 100-ms acquisition reduces the motion effects seen in Figures 4a,b, compared to Figures 3a,b acquired with the longer 200-ms acquisition window. However, Figures 4a,b and Figures 4c,d require 43 cardiac cycles and 22 cardiac cycles respectively, each of which are longer than the 11 cardiac cycles required for sufficient image quality, Fig. 3d.

4 Summary and Conclusion

We have demonstrated the capability of a numerical simulation environment to simulate different acquisition and gating strategies. This numerical environment will assist in the development of an intra-operative 3D coronary angiography system for use during minimally invasive CAB procedures. To simulate 3D coronary angiography we have implemented a forward projection algorithm, in combination with a dynamic model to create 2D projections using different gating acquisition strategies. The 2D projections are then reconstructed to create a simulated 3D CT image. Results from this preliminary study indicate that acquisition windows of 100-200 ms produces good-quality 3D angiograms. This acquisition window is similar to those used with retrospectively gated multi-slice spiral CT scanners.

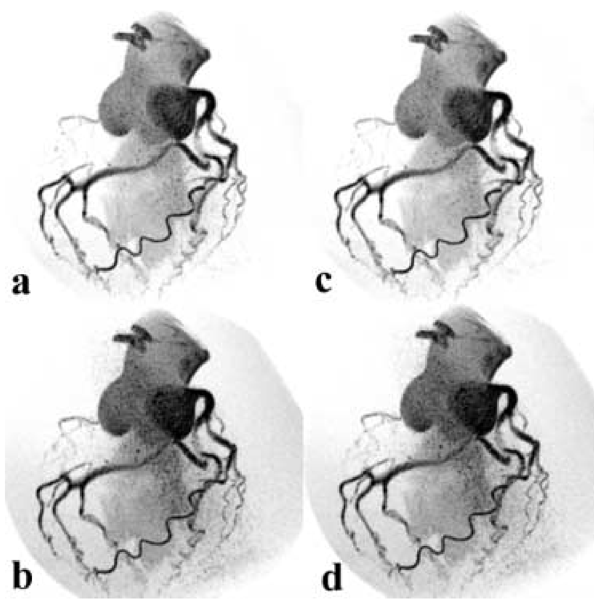

Fig. 4. MIPs through the volumes created using gating strategy (II), a 100-ms acquisition window. Shown are (a) 129 views, and (b) 65 views acquired during early diastole, and (c) 129 views, and (d) 65 views acquired during mid diastole.

The data presented here were based on a specific dynamic model of the coronary circulation. However, there is great diversity among the patient population undergoing minimally invasive CAB procedures. To better simulate 3D coronary angiography, our future work will include extracting the motion of different human hearts to allow a variety of different gating strategies to be tested for both healthy and diseased hearts. Further studies will also include quantifying image quality, as well as ROC analysis to determine the optimum method for obtaining 3D coronary angiograms using intra-arterial injections during intra-vascular therapy procedures. These encouraging studies have indicated that it should be feasible to develop a gated acquisition strategy that can be used to acquire intra-operative 3D coronary angiograms. These angiograms can be incorporated within the VCSP for assisting initial placement of the ports and instruments, intra-procedure verification of port and instrument placement and the success of a bypass graft in MIRCAB procedures.

Acknowledgments

We acknowledge Drs. A.J. Dick and M. Quantz for their clinical assistance, Chris Norley and Hristo Nikolov for their help acquiring the CRA images, as well as David Gobbi for the helpful discussions. Partial financial support for this work from the Canadian Institutes for Health Research and the Heart and Stroke Foundation of Canada is gratefully acknowledged.

References

1. Chiu AM, Dey D, Drangova M, *et al.* "3-D Image Guidance for Minimally Invasive Robotic Coronary Artery Bypass." *Heart Surg Forum* **3**, 224-31 (2000).
2. Lehmann G, Chiu A, Gobbi D, *et al.* "Towards dynamic planning and guidance of minimally invasive robotic cardiac bypass surgical procedures" *MICCAI* (2001).
3. Fahrig R, Fox AJ, Lownie S, *et al.* "Use of a C-arm system to generate true three-dimensional computed rotational angiograms: preliminary in vitro and in vivo results" *AJNR Am J Neuroradiol* **18**, 1507-14 (1997).
4. Fahrig R and Holdsworth DW. "Three-dimensional computed tomographic reconstruction using a C-arm mounted XRII: image-based correction of gantry motion nonidealities" *Med Phys* **27**, 30-8 (2000).
5. Lehmann GC, Gobbi DG, Dick AJ, *et al.* "Dynamic Three-Dimensional Model of the Coronary Circulation" *Proc. SPIE Med. Imaging* (2001).
6. F.L. Bookstein. "Principal warps: Thin-plane splines and the decomposition of deformations" *IEEE Trans Pattern Analysis and Machine Intelligence,* **PAMI-1**, 567-85 (1989).
7. Python programming environment. www.python.com.
8. Atamai Inc. www.atamai.com.
9. The Visualization Tool Kit (VTK). www.kitware.com .
10. Siddon RL. "Fast Calculation of the exact radiological path for a three-dimensional CT array" *Med. Phys.* **12**, 252-5 (1985).
11. Feldkamp LA, Davis LC, and Kress J.W. "Practical cone-beam algotithm" *J. Opt. Soc. Am.* **1**, 612-9 (1984).